Charles University

1st Faculty of Medicine

Institute of Clinical Biochemistry and Laboratory Diagnostics

Laboratory of Hepatology

The role of glycoconjugates in cell signalling - CEACAM1 and FcεRI

Ph.D. basis thesis

2006 **Mgr. Lenka Dudková**

Author: Mgr. Lenka Dudková
Address: Laboratory of Hepatology, ÚKBLD 1.LF UK a VFN
U nemocnice 2, 128 00 Czech Republic
Telephone: +420 224 962 559
E-mail: dudkova@cesnet.cz
Commission: Biochemistry and Pathobiochemistry
Supervisor: doc. RNDr. František Šmíd, CSc.
Opponents:

Ph.D. thesis sent:
Defense of Ph.D. thesis:
Place of defence:

Chairman of the Biochemistry and Pathobiochemistry commission:
Prof. MUDr. Jiří Kraml, DrSc.
Institute of Medical Chemistry and Biochemistry
1st Faculty of Medicine, Charles University
Kateřinská 32, Prague 2

Ph.D. thesis was elaborated within the postgraduate program for studies in Biomedicine at the Laboratory of Hepatology, Institute of Clinical Biochemistry and Laboratory Diagnostics, General University Hospital and 1st Faculty of Medicine Charles University in Prague. This work was supported by the grant projects IGA-MZ ČR 4046-3 from the Ministry of Health and GA ČR 204/00/0204 from the Czech Science Foundation.

Contents

1. Introduction

Carcinoembryonic antigen adhesion molecule 1 (CEACAM1) is a human membrane glycoprotein belonging to the carcinoembryonic antigen (CEA) family and to the immunoglobulin superfamily. It is expressed in apical membranes of many epithelial cells in the gastrointestinal and urogenital tract and also in granulocytes and lymphocytes [1]. Little is known about the function of CEACAM1. The role of CEACAM1 as a cell adhesion molecule was described first and proved subsequently in numerous *in vitro* studies. The role in signal transduction, its regulation, tumour cell growth regulation, apoptosis, angiogenesis and apical membrane organisation have recently been discussed in the literature [2, 3, 4]. This glycoprotein could influence aggregation of biliary vesicles in supersaturated bile and thus speed up cholesterol crystallisation and bile stone formation [5]. There are two isoforms of CEACAM1 present in normal human bile, known as CEACAM1-85 and CEACAM1-115, according to their apparent molecular weights on SDS–PAGE gel.

It was necessary to isolate CEACAM1 from human bile for our studies and verification of our hypotheses. CEACAM1 was isolated from human bile by protein extraction with perchloric acid, ion-exchange chromatography followed by concanavalin A-Sepharose affinity chromatography and gel filtrations on Sephadex G200 and Sephacryl S200 or Sepharose 4B [6]. Immunoaffinity chromatography was also used for isolation of CEACAM1 and other CEA-related antigens from bile [7]. None of the above mentioned papers gave any information about the yield and purity of the isolated proteins.

To isolate enough amount of pure CEACAM1 from bile for our studies we prepare a simple immunoaffinity method based on oriented immobilisation of the monoclonal anti-CEA antibody on hydrazide-derivatised cellulose.

Gangliosides are a family of sialic acid-containing glycosphingolipids located almost exclusively in the outer leaflet of the plasma membrane. The carbohydrate moiety of gangliosides can mediate cell-cell or cell-matrix interactions that regulate cell growth, cell differentiation, and signal transduction in various cell types [8]. Since gangliosides are amphiphilic molecules, they have the capability of binding to biological membranes when added exogenously. It was previously suggested that this property could be involved in the immunosuppressive activity of gangliosides shed from tumour cells. Exogenously added brain or tumour gangliosides are capable of inhibiting a variety of immune responses,

proliferation, differentiation and secretory responses [9]. The mechanism whereby isolated gangliosides modulate the immunoreceptor-mediated signalling is poorly understood. They could interact directly with plasma membrane receptors or affect the overall structure of the plasma membrane, in particular the properties of glycosphingolipid-enriched membranes (GEM), also called lipid rafts. The latter possibility is strengthened by data indicating that exogenously added gangliosides could displace GPI-anchored proteins from lipid microdomains [10]. Changes in membrane gangliosides could therefore affect the immunoreceptor signalling because GEM have been suggested to function as platforms for spatial organisation of signal transduction molecules [11].

In mast cells, the first biochemical event detectable after FcεRI aggregation is tyrosine phosphorylation of the FcεRI β and γ subunits by protein tyrosinekinase (PTK) Lyn. This process creates new binding sites for Lyn and Syk PTK through Src homology-2 (SH2)-mediated interactions with phosphotyrosine residues of immunoreceptor tyrosine-based activation motifs (ITAM). Activation of these newly recruited kinases, in turn, facilitates the translocation and phosphorylation of multiple substrates, including the linker for activation of T cells (LAT) and phospholipase C (PLC)γ isozymes. These proteins interact to form a functional macromolecular signalling complex at the plasma membrane. Activated PLC catalyses the cleavage of the lipid substrate phosphatidylinositol 4,5-bisphosphate (PIP2) into diacylglycerol, a stimulator of protein kinase C, and inositol 1,4,5-trisphosphate (IP3), a ligand for the IP3 receptor Ca^{2+} channel in the endoplasmatic reticulum membrane that induces a rise in cytoplasmic Ca^{2+} levels. An important intermediate in this pathway is phosphatidylinositol 3-kinase (PI3K) which catalyses the synthesis of phosphatidylinositol 3,4,5-trisphosphate (PIP3) and phosphatidylinositol 3,4-bisphosphate. All these events result in a formation of large signalling complexes responsible for further propagation of the activation signal [12].

In this study, we investigated at which step the gangliosides interfere with FcεRI-mediated signalling. We used the rat basophilic leukaemia (RBL-2H3) cell line as a model for analyses of the effects of gangliosides on GEM function in early stages of mast cell signalling.

2. Aims

1. To develop an affinity chromatography method to isolate CEACAM1 from human bile in sufficiently amount and purity for followed experiment with this glycoprotein.

2. To investigate how exogenous gangliosides interfere with FcεRI mediated signalling.

3. Methods

3.1. Preparation of immunoaffinity column and isolation of CEACAM1 from bile

Monoclonal antibody F34-187 [13] was solubilised in 0,1 M acetate buffer, pH 5,5, 0,1 ml of 0,1 M sodium periodate was added and the antibody was oxidised for 20 min at 4 °C with shaking. Dialysed antibodies were added to hydrazide cellulose and incubated for 24 h at 4 °C. Four amino acid contents (alanine, glycine, asparagine and threonine) were used for calculation of percentage of the immobilised antibody from the amount of antibody used for immobilisation (Biochrom amino acid analyser, Pharmacia, Sweden).

The crude protein extract was prepared by perchloric acid extraction as described by Neumaier et al. [7] from 2500 ml of bile obtained via external drainage from the patient with benign postcholecystectomic stenosis of the bile duct. The extract was neutralised, dialysed, concentrated and lyophilised. The appropriate amount of the crude protein fraction (see results) was dissolved in PBS, incubated with immobilised antibody and applied onto the column. The non-bound fractions were eluted with 400 ml PBS, the bound antigens were then eluted with 6 M guanidine-HCl in PBS and 15 ml fractions were collected.

All the fractions obtained from the affinity chromatography were dialysed, lyophilised, dissolved in reducing sample buffer and analysed by SDS-PAGE followed by immunoblott with polyclonal rabbit anti-CEA antibody (DAKO, Denmark) or lectin staining with concanavalin A-HRP (Sigma-Aldrich, USA) according to the method of Laemmli and Towbin et al. [14, 15]. The non-specific protein staining with Coomassie brilliant blue G,

silver stain kit, amidoblack, sypro orange, sypro red and sypro tangerine (Molecular Probes, USA) was performed according to manufacturers' instructions. Quantification of proteins was done by the fluorescamine method according to the standard protocol.

3.2. Methods used for the study of the signalling pathways of FcεRI

3.2.1. Cell activation, immunoprecipitation and immunobloting

RBL-2H3 (rat basophilic leukaemia) cells were cultured as described [16]. The cells were harvested, resuspended at a concentration of $1{,}5x10^6$ cells/ml in G-medium supplemented with or without 50 μM brain gangliosides and incubated for 20 h as monolayer. Gangliosides-pretreated and control cells were harvested, resuspended in G-medium at a concentration 10^7 cells/ml and sensitised in a suspension with IgE (IGEL b4 1; 1000 x diluted ascites) or biotinylated OX7 mAb (3 μg/ml). After 30 min at 37 °C in 5 % CO_2 in air, the cells were washed in BSS supplemented with 0,1 % BSA and activated at 37 °C by exposure to TNP-BSA (1 μg/ml) or streptavidin (10 μg/ml). In cells activated via FcεRI dimers, the sensitisation step was omitted and the cells were directly activated by 5.14 mAb anti FcεRI α subunit. β-glucuronidase released (degranulation) into supernatant was measured as described [17, 18]. The cell pellets were lysed in a ice-cold lysis buffer containing 50 mM Tris-HCl (pH 7,4), 150 mM NaCl, 2 mM EDTA, 10 mM β-glycerophosphate, 1 mM Na_3VO_4, 1 mM PMSF, 1 μg/ml aprotinin, 1 μg/ml leupeptin and supplemented with 1 % NP-40 and 1 % n-dodecyl β-D-maltoside (LAT, Syk and PLC γ IP) or 0,2 % Triton X-100 (FcεRI IP). Post nuclear supernatants were IP with corresponding antibodies prebound to UltraLink-immobilised Protein A (Pierce), size fractionated by SDS-PAGE and immunoblotted with the corresponding antibodies as described [19]. Aliquots of post nuclear supernatants (corresponding to $0{,}25x10^6$ cells) were examinated for tyrosine phosphorylation in whole cell lysate proteins.

3.2.2. Sucrose density gradient fractionation

Labelling of mAb with ^{125}I (ICN biomedicals, USA) by chloramine-T method and isolation of GEM by sucrose density gradient ultracentrifugation has been described [20].

3.2.3. PIP3 and IP3 determination

PIP3 was detected by a modification of a previously described procedure [21] adapted for the microcentrifuge tubes. Briefly, cells at a concentration 10^7/ml in BSS/BSA were incubated with 200 μCi/ml [^{32}P]orthophosphate (Amersham Pharmacia Biotech, UK) for 1 h at 37 °C before stimulation with TNP-BSA. The reaction was stopped by centrifuging and resuspending the pellet in 500 μl of ice-cold methanol : chloroform (2:1, v/v) followed 350 μl of ice-cold chloroform and 350 μl of 1,2 M HCl. The tubes were vortexed, centrifuged, and the organic phase (400 μl) was reextracted with 400 μl of methanol : 0,6 M HCl (1:1, v/v). After centrifugation the organic phase (300 μl) was dried, resuspended and applied to thin-layer chromatography Silica gel-60 plates (Merck, Germany) precoated with potassium oxalate (1,2 % in 40 % methanol). Chromatography was performed in a mixture of chloroform : acetone : methanol : acetic acid : water (80:30:26:24:14, all v/v). Radioactive phospholipids were detected by autoradiography and quantified by densitometry. Phosphoinositides (Sigma and Matreya, USA) of known composition were used as a standard and detected by exposing the plates to iodine vapours.

IP3 was determined as described by [22]. Briefly, $6x10^6$ RBL-2H3 cell pretreated or not with gangliosides were sensitised with IgE (anti TNP) and stimulated with TNP-BSA in 500 μl BSS/BSA. At various time intervals the reactions were terminated by adding 100 μl of ice-cold trichloracetic acid (100 %). IP3 was extracted from the samples and quantified using a commercially available assay kit (PerkinElmer, USA).

3.2.4. Calcium mobilisation

Changes in the concentration of free intracellular Ca^{2+} ($[Ca^{2+}]_i$) in ganglioside-pretreated or control cells were determined using Fluoro-3-AM or Fura Red-AM probe (Molecular Probes, USA) as previously described [20, 23, 24, 25].

3.2.5. F-actin assay

Total amount of polymeric actin was determined as previously described [26]. Briefly, to 200 µl of the cell suspension (10^6 cells) in BSS/BSA was added 300 µl of PBS containing 50 µg lysophosphatidylcholine (Sigma), 6 % formaldehyde and 0,125 µg of FITC-labelled phalloidin (Sigma). After incubation for 10 min at 37 °C the cells were centrifuged, resuspended in PBS and analysed by flow cytofluorometry using FACSCalibur (Becton Dickinson, USA).

3.2.6. Immune complex PI3K and PLCγ assays

PI3K activity was measured as previously described with minor modifications [27]. FcεRI-activated or control RBL-2H3 cells ($2x10^6$) were solubilised in 500 µl lysis buffer (20 mM Tris-HCl (pH 8,0), 137 mM NaCl, 2 mM EDTA, 1 mM Na_3VO_4, 1 mM PMSF, 10 µg/ml aprotinin and leupeptin) supplemented with 1 % Triton X-100. PI3K in post nuclear supernatants was immunoprecipitated with anti-PI3K p85 subunit Ab and the immunocomplexes were collected on UltraLink immobilised protein A (10 µl). The beads were washed twice with lysis buffer supplemented with 0,1 % Triton X-100, twice with kinase assay buffer (20 mM HEPES (pH 7,4), 20 mM $MgCl_2$ and 0,25 mM EGTA), and then suspended in 25 µl kinase buffer with or without 100 nM wortmannin. After 10 min at 25 °C, PI3K assay was initiated by an addition of 25 µl of kinase buffer containing 10 µg of sonicated phosphatidylinositol (Sigma-Aldrich) and 37 kBq [γ-^{32}P]ATP (Amersham Pharmacia Biotech; final concentration 10 µM) and the reaction mixture was incubated for 30 min at 25 °C. During this period, the formation of phosphatidylinositol phosphate was linear (data not shown). The reaction was terminated by adding 250 µl

methanol : chloroform (2:1, v/v), chloroform (175 µl), and 1,2 M HCl (175 µl). The organic phase was extracted again with 200 µl methanol : 0,6 M HCl (1:1, v/v) and lyophilised. Lipids were resuspended in 15 µl of chloroform : methanol (1:1, v/v), spotted on TLC Silica gel-60 plate (Merck), precoated with potassium oxalate and resolved in chloroform : methanol : 4 M ammonium hydroxide (9:7:2, v/v/v) for 1 h. ^{32}P-labelled materials were visualised by autoradiography and quantified by Fuji Bio-Imaging Analyzer Bas 5000 (Tokyo, Japan).

PLCγ assay was performed essentially as described [28]. FcεRI-activated or control RBL-2H3 cells were solubilised in a lysis buffer (20 mM HEPES (pH 7,5), 150 mM NaCl, 5 mM β-glycerophosphate, 0,2 mM Na_3VO_4, 1 mM EGTA, 1 mM PMSF, 1 µg/ml aprotinin, and 1 µg/ml leupeptin) supplemented with 1 % Triton X-100. PLCγ1 or PLCγ2 in post nuclear supernatants were immunoprecipitated with the corresponding antibodies and the immunocomplexes were bounded on UltraLink immobilised protein A. The beads (15 µl) were washed and then suspended in 25 µl reaction buffer. After addition of 10 µl substrate solution containing 25 mM sodium phosphate (pH 6,8), 50 mM KCl, 2,5 % Triton X-100, 6 µg of PIP2 and 1,1 kBq of P[^{3}H]IP2 (PerkinElmer), the beads were incubated for 30 min at 35°C. TCA precipitates were removed by centrifugation and the supernatants collected for quantification of the released [^{3}H]IP3 by liquid scintillation counting. Immunocomplexes bound to the pelleted beads were solubilised in SDS-PAGE sample buffer and analysed by immunoblotting for the presence of PLCγ.

3.2.7. Statistical analysis

Data are expressed as means ± SD. Statistical analysis was performed by two-tail unpaired Student's t-test and $p < 0,05$ was considered statistically significant.

4. Results

4.1. Isolation of CEACAM1 from bile

The affinity column 2,0 (i.d.) × 4,5 cm, bed volume 14 ml, was used for preparative chromatography and obtained data were recalculated per 1 ml of the gel volume. We immobilised 0,75 mg of mAb F34-187 anti-CEA per ml of hydrazide cellulose. The actual amount of the immobilised antibody was determined using analysis of amino acids and this method was compared with the UV spectrophotometry (280 nm). Using amino acid analysis, four amino acids that are completely released after 24 h hydrolysis (alanine, glycine, threonine and asparagine) were used for calculation. From obtained values it was calculated that approximately 0,3 mg of antibody per ml of hydrazide cellulose were immobilised from originally used 0,75 mg per ml. The higher amount (0,6 mg/ml) was obtained when the UV spectrophotometry was used.

About 1,27 g of lyophilised crude protein fraction enriched with CEACAM1 was obtained from 2500 ml of human bile by extraction with perchloric acid. Samples of 2,9 mg and 5,6 mg of the crude protein fraction per ml of hydrazide cellulose were loaded onto the column. The recovery of the eluted protein was 135 ± 49 and 361 μg/ml bed volume, respectively, as determined by spectrofluorometry (for details see Table 1). Higher load of the protein extract did not lead to the increase of recovery of isolated protein.

The aliquot of protein sample loaded onto the affinity column, the aliquots of the non-bound fractions washed out from the column and the fractions eluted with 6 M guanidine hydrochloride were analysed by SDS-PAGE and immunoblott with the polyclonal rabbit anti-CEA antibody (Dako, Denmark). A single 85 kDa band of non-bound glycoprotein could be detected in the original sample and in the first washing fractions. No immunopositivity was found in last washing fraction Wx, but a strong signal appeared again in the fractions E1-E3 eluted with guanidine-HCl, see Figure 1.

In order to detect other protein bands possibly presented in the sample of immunopurified CEACAM1, the following methods of non-specific protein staining were tested: silver staining, Coomassie brilliant blue, Sypro orange, Sypro red, Sypro tangerine and amidoblack and India ink. With these methods, we were able to detect multiple protein

bands in the crude protein but no bands could be visualised in the affinity-purified fractions E1-E3. The only band that could be silver stained in the affinity purified fractions when higher amounts of protein were loaded onto the gel was that of albumin. The immunopurified CAECAM1-85, which appeared to be the most abundant biliary isoform of CEACAM1 present in the fraction according to immunochemical staining, did not stain at all. The only method which could detect the 85 kDa band was staining with concanavalin A-HRP on the blot followed by the ECL kit (Amersham Pharmacia Biotech), see Figure 2.

Table 1: Experimental data obtained from affinity chromatography

Column No.	1	2
Column i. d. × column length (cm)	2,0 × 4,5	2,0 × 4,5
Bed volume (ml)	14	14
Concentration of mAb loaded (mg/ml bed)	0,75	0,75
Concentration of the immobilised mAb based on amino acid analysis (mg/ml bed)	0,3	0,3
Concentration of the immobilised mAb based on UV spectrometry (mg/ml bed)	0,6	0,6
Crude extract load (mg/ml bed)	2,9	5,6
Recovered CEACAM1(µg/ml bed)	135 ± 49	361
Recovered CEACAM1 (%)	4,66	6,45

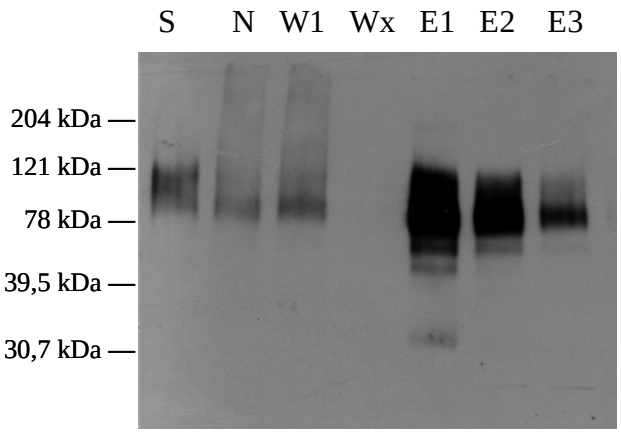

Figure 1: Immunostaining (with anti-CEA polyclonal antibody) of fractions from affinity column after SDS-PAGE. S - aliquot of protein sample isolated by extraction with TCA. **N** - non-bound protein also containing small amount of unbound immunopositive protein. Non-bound protein was washed out in several fractions (see **W1**). No immunopositive band was observed in the last fraction after extensive washing with 400 ml of PBS (**Wx**). Change of the washing buffer for 6 M guanidine hydrochloride led to the elution of immunopositive protein in fractions **E1-E3**.

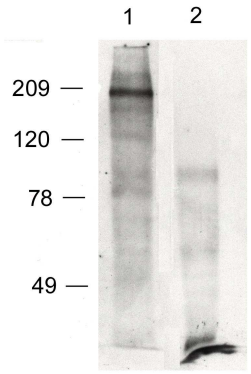

Figure 2: Lectin staining of crude protein after extraction with perchloric acid (lane **1**) and of the immunopurified CEACAM1 (lane **2**). The membrane was blocked with 50 mM Tris-HCl containing 0,15 M NaCl and 0,01 % Tween-20 for 1 h, incubated with concanavalin A-peroxidase (2 mg/ml) in a similar buffer containing 0,5 M NaCl for 1 h, washed 3 × 10 min with the blocking buffer, and detected with ECL kit. 6,25 μg of the total protein was loaded onto each lane.

4.2. Exogenous administration of gangliosides inhibits FcεRI-mediated mast cell degranulation by decreasing the activity of phospholipase Cγ

4.2.1. Exogenously added gangliosides selectively inhibit the FcεRI mediated secretory response

A preincubation of RBL-2H3 cells with highly purified human brain gangliosides inhibited the β-glucuronidase release induced by antigen-mediated aggregation of IgE-FcεRI complexes (Figure 3*A*). Pilot experiments indicated that the maximum inhibition was observed after incubation of the cells for 20 h with gangliosides at a concentration 50 μM in G-medium. Under these conditions, gangliosides did not exhibit any cytotoxic effect as determined by trypan blue dye exclusion test. A similar inhibitory effect was observed when the FcεRI was aggregated by anti-FcεRI mAb 5.14 (Figure 3*B*). The inhibitory effect was specific for FcεRI-mediated activation, because it was absent in Thy-1 glycoprotein activated cells, which responded even more than control cells (Figure 3*C*). The maximal inhibitory effect was seen at an antigen concentration that gave a maximum secretory response in control cells (1 μg/ml; Figure 3*D*).

Gangliosides present in the human brain differ in their sialic acid and carbohydrate chain moieties. To determine whether the inhibitory effect is confined to specific gangliosides, we compared the effect of monosialoganglioside GM1, asialo-GM1, disialoganglioside GD1a and trisialoganglioside GT1b on FcεRI-mediated secretory response. Preincubation of the RBL-2H3 cells with GM1 significantly inhibited the secretory response although the inhibition was weaker compared with brain gangliosides (Figure 3*E*). Interestingly, asialo-GM1 inhibited the secretory response to a similar extent as GM1, suggesting that sialic acid had no significant role in the inhibitory effect of GM1. Pretreatment with GT1b and GD1a, the dominant brain gangliosides, resulted in a decrease of the secretory response, which was comparable to the inhibition observed after pretreatment with isolated brain gangliosides. Because of these results, isolated brain gangliosides were used in most experiments.

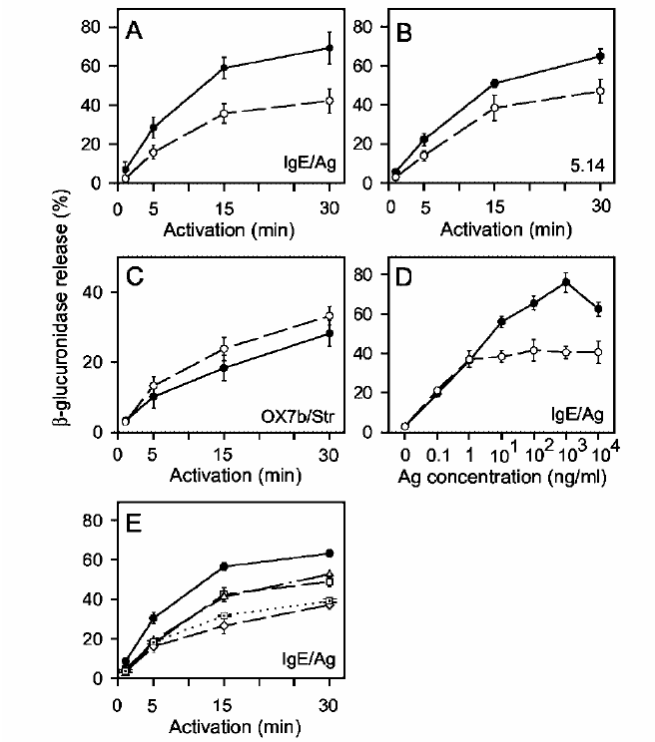

Figure 3: Exogenously administered gangliosides selectively inhibit FcεRI-mediated secretion. *A–D*, RBL-2H3 cells were incubated for 20 h with 50 μM isolated brain gangliosides in G-medium (○) or with G-medium alone (●). After incubation, the cells were sensitised for 30 min with TNP-specific IgE (*A* and *D*), biotinylated anti-Thy-1.1 mAb OX7 (*C*), or not sensitised (*B*). The cells were activated by aggregation of the IgE-FcεRI complexes by TNP-BSA (*A*; 1 μg/ml), dimerisation of FcεRI by 5.14 mAb (*B*; 1 μg/ml) or aggregation of Thy-1-biotinylated OX7 complexes by streptavidin (Str; 10 μg/ml; *C*). The amount of β-glucuronidase released into the supernatant was determined at various time intervals. In *D*, IgE-sensitised cells were stimulated with various concentrations of TNP-BSA, and β-glucuronidase was determined after 30 min. In *E*, the cells were pretreated for 20 h with G-medium supplemented with 50 μM GT1b (◇), GD1a (⊡), GM1 (□), asialo-GM1 (△) or in G medium alone (●), and activated as in *A*. Means ± SD of 4 (*A–D*) or 2 (*E*) independent experiments performed in duplicates or triplicates are presented.

Gangliosides-pretreated cells, compared with control cells, exhibited a decreased adhesion to the substratum, with a more rounded morphology and with less developed processes (Figure 4, *A* and *B*). Similar changes in cell morphology were observed in cells pretreated with GT1b, GD1a, GM1 and asialo-GM1 (not shown). These changes were associated with the decreased amount of F-actin observed in nonactivated gangliosides-pretreated cells (inhibition 17 ± 7%; mean ± SD; $n = 5$; $p < 0{,}01$). After antigen-mediated activation, the amount of F-actin was significantly higher in both gangliosides-pretreated and

control cells. In the former, however, the levels of F-actin remained lower at all time intervals analysed (Figure 4*C*).

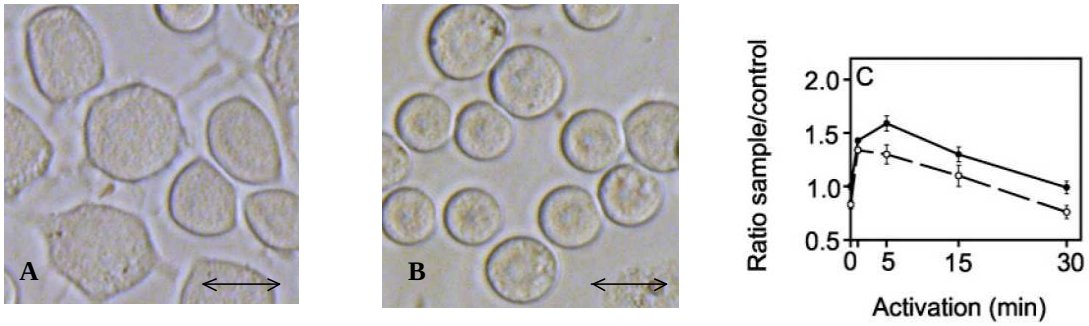

Figure 4: Morphology and F-actin of ganglioside-pretreated cells. RBL-2H3 cells were incubated with isolated brain gangliosides in G-medium (*A*) or in G-medium alone (*B*). Phase contrast images were taken after 20 h. Bar = 10 µm. *C*, The amount of F-actin in ganglioside-pretreated (○) or control cells (●) was determined by flow cytofluorometry in IgE-sensitised cells activated for various time intervals by TNP-BSA (1 µg/ml). Means ± SD were calculated from five independent experiments.

4.2.2. Gangliosides do not prevent the association of aggregated FcεRI with GEM

When aggregated, the FcεRI rapidly associate with GEM [29]. Because it has been shown that brain gangliosides interfere with the integrity of GEM [10], we further analysed the solubility of FcεRI in cells exposed to isolated gangliosides. Our data indicate that the majority of nonaggregated FcεRI from both control and gangliosides-pretreated cells solubilised in 0,06 % Triton X-100 was located in the high-density fractions of sucrose gradient (>35 % sucrose) and after aggregation most of the IgE-FcεRI complexes from both control and treated cells were found in the low-density fractions (15-35 % sucrose). However, a significant amount of FcεRI was still found in the high-density fractions (>55% sucrose); it probably represents the cytoskeleton bound aggregated FcεRI, which differs from the GEM-associated FcεRI. It could be concluded that gangliosides had no significant effect on this association. Thus, the observed inhibitory effect of gangliosides on FcεRI-mediated secretion in RBL-2H3 cells does not seem to be a direct consequence of reduced association of aggregated FcεRI with GEM or displacement of GPI-anchored proteins from GEM.

4.2.3. Decreased tyrosine phosphorylation and enzymatic activity of PLCγ in gangliosides pretreated cells

In an attempt to determine whether exogenous gangliosides inhibit early FcεRI-mediated signalling events we further analysed tyrosine phosphorylation of FcεRI, Syk, LAT and PLCγ. Tyrosine phosphorylation of FcεRI β and γ subunits, Syk PTK and LAT was not inhibited by pretreatment with gangliosides. In fact, tyrosine phosphorylation of LAT was increased in antigen-activated cells in all 3 performed experiments (+46,6 ± 11,6 %). Although PLCγ1 and PLCγ2 from both gangliosides-pretreated and control cells bound to LAT comparably (Figure 5*B*), their tyrosine phosphorylation was significantly reduced (Figure 5*A*). These data suggested that exogenous gangliosides could affect activity of PLCγ.

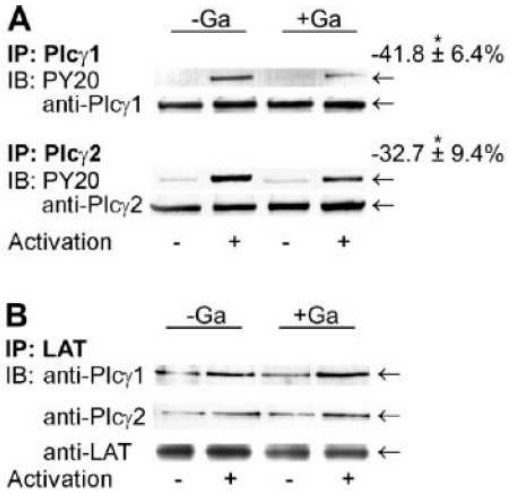

Figure 5: Tyrosine phosphorylation and interaction of PLCγ. RBL-2H3 cells were incubated with isolated brain gangliosides in G-medium (+Ga) or in G-medium alone (-Ga), sensitised with IgE and activated (+) or not (-) with TNP-BSA (1 μg/ml). *A,* Tyrosine phosphorylation of PLCγ1 and 2 was detected by phosphotyrosine immunoblotting (IB) with PY20 mAb (Transduction Laboratories, USA) after IP. The quantity of proteins in IP was assessed by immunoblotting with appropriate antibodies on stripped membranes. The relative amount of tyrosine phosphorylated proteins of ganglioside pretreated and stimulated cells are given in percent of stimulated controls. *B,* Association of LAT with PLCγ1 and PLCγ2 was determined after IP of LAT followed by immunoblotting with PLCγ1; PLCγ2 and LAT antibodies. Similar results were obtained in three independent experiments. Arrows indicate position of the corresponding proteins.

Full activation of PLCγ requires its membrane recruitment by an interaction with LAT and PI3K lipid products [30]. Major function of PLCγ there is to hydrolyse PIP2 to IP3 and diacylglycerol, which induce the release of Ca^{2+} from intracellular stores and the

activation of protein kinase C (PI3K), respectively. The primary in vivo substrate of PI3K is PIP2, which is converted to PIP3. In additional experiments we measured the levels of PIP3 in the course of the activation of gangliosides pretreated as well as control cells. In gangliosides pretreated cells the baseline level of PIP3 was decreased and these levels were also significantly lower in antigen-activated cells, compared with cells cultured in media without gangliosides (time 0). It should be noted that exogenously added gangliosides also reduced the baseline PIP2 levels (inhibition 21 ± 8 %; mean ± SD; n = 4; $p < 0.05$). The differences between control and gangliosides pretreated cells after antigen triggering were not significant (Figure 6*A* and *B*).

The observed decrease in PIP3 levels could be the result of a decreased activity of PI3K, an increased activity of the corresponding phosphatases and/or a decreased availability of PI3K substrate. In additional experiments, we therefore evaluated the PI3K activity by immunocomplex kinase assay. PI3K was IP from control or gangliosides pretreated cells activated for various time intervals with antigen. Data presented in Figure 6*C* indicate that control cells incubated for 20 h in the absence of gangliosides exhibited a relatively rapid increase in PI3K activity after exposure to antigen (2,5-fold increase in 15 s) which declined after 5 min. Pretreatment with gangliosides did not inhibit PI3K activity but resulted instead in its increase, especially at early time intervals after the exposure to antigen. A significant increase of PI3K activity was also observed after pretreatment of the cells with GD1a and GT1b gangliosides, the major components of brain gangliosides (Figure 6*C*). As expected, pretreatment of PI3K immunocomplexes with 100 nM wortmannin completely inhibited the formation of ^{32}P labelled PIP. These data indicate that the observed decrease in PIP3 levels in gangliosides-pretreated cells is not due to a decreased activity of PI3K.

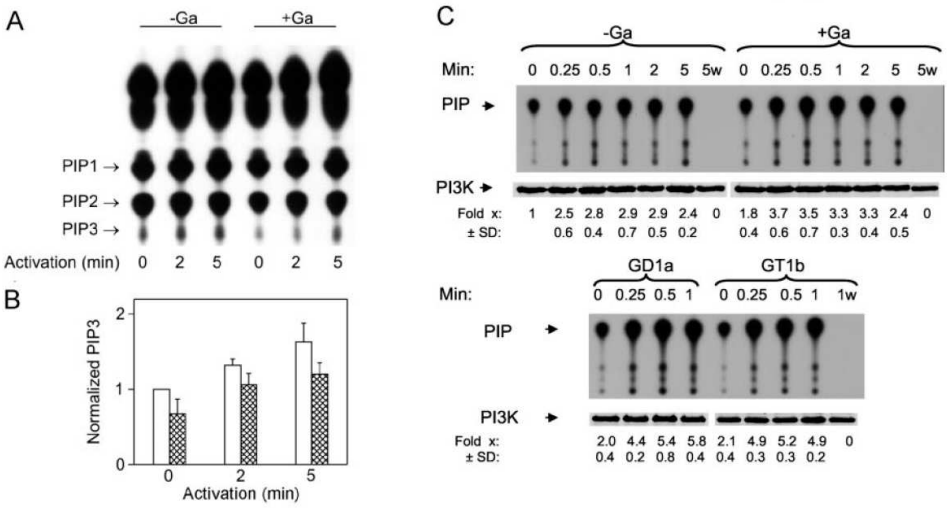

Figure 6: PIP3 levels and activity of PI3K in gangliosides pretreated and antigen-stimulated cells. *A* and *B*, RBL-2H3 cells were incubated in the presence (+Ga) or absence (-Ga) of isolated brain gangliosides and then sensitised with IgE. PIP3 levels were measured in [^{32}P]orthophosphate-labelled cells before (0 min) and following stimulation with TNP-BSA (1 μg/ml). The TLC separation pattern was determined using phosphoinositide standards. A representative TLC is shown (*A*). Quantitative measurement of PIP3 level, corrected for the total signal from phosphatidylinositol monophosphates PIP1, PIP2 and PIP3, in controls (☐) or ganglioside pretreated cells (▩) was determined by densitometry of films (*B*). Data are presented as means ± SD, calculated from four independent experiments, and normalised to nonstimulated control cells. *C*, PI3K enzymatic activity was measured in cells preincubated with G-medium alone (-Ga) or G-medium supplemented with 50 μM brain gangliosides (+Ga), GD1a or GT1b. The cells were stimulated with antigen for various time intervals and PI3K activity was determined as described in 3.2.3. Samples labelled 5w and 1w were from cells stimulated with antigen for 5 min and 1 min and the immunocomplexes were exposed for 10 min to 100 nM wortmannin before PI3K assay. Migration of PIP is indicated by arrow. Representative results are shown on top panels. Quantitative measurements of PIP were normalised to unstimulated control cells and to the amount of PI3K detected by immunoblotting of whole cell lysates. Means of fold increase ± SD were calculated from three to five independent experiments.

Decreased tyrosine phosphorylation of PLCγ1 and PLCγ2 in gangliosides pretreated cells suggested their reduced enzymatic activity. To prove that the activity of PLCγ is indeed reduced, we measured the PLCγ activity in an immunocomplex assay. In control cells preincubated in G-medium alone, the activities of PLCγ1 and PLCγ2 were increased ~6-fold and 8-fold, respectively, after 1 min exposure to antigen, and then declined (Figure 7*A* and *B*). Pretreatment with gangliosides inhibited the activity of both enzymes at all time intervals analysed. The observed inhibition was not due to decreased levels of the enzymes as could be inferred from the results of immunoblotting analyses of PLCγ1 and PLCγ2 IP from control and gangliosides pretreated cells (not shown).

Our findings that gangliosides inhibit the activity of PLCγ were supported by measurements of IP3 levels in control and gangliosides pretreated cells after stimulation with antigen (Figure 7*C*). In control cells, antigen stimulation induced a rapid augmentation of IP3 concentrations, with a peak at 15 s, followed by a slow return to baseline levels. In gangliosides-pretreated cells, the baseline level of IP3 was comparable to that in control cells at time 0 min, but was significantly reduced after stimulation with antigen (Figure 7*C*). The reduced IP3 levels in gangliosides-pretreated and activated cells were reflected in a decreased calcium response after activation in media supplemented with Ca^{2+} (Figure 7*D*), as well as in the absence of Ca^{2+} (Figure 7*E*). Exogenously added gangliosides had no effect on Ca^{2+} response induced by calcium ionophore A23187 (Figure 7*F*), suggesting that the signal transduction pathways involving PLCγ, rather than Ca^{2+} channels, are modulated by gangliosides.

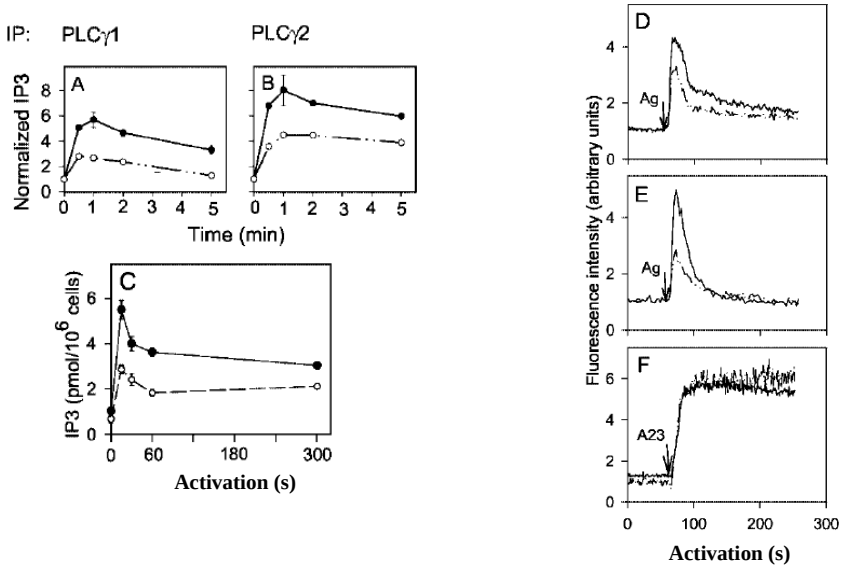

Figure 7: Exogenously administered gangliosides inhibit the enzymatic activity of PLCγ, and Ca^{2+} mobilisation in antigen-activated cells. RBL-2H3 cells were incubated in the presence (○) or absence (●) of isolated brain gangliosides and then sensitised with IgE. *A* and *B)* Enzymatic activities of PLCγ1 and PLCγ2 were measured by immune complex PLC assay as described in 3.2.3. Cells were collected before or at various time intervals after stimulation with TNP-BSA. Means ± SD were calculated from two to three experiments performed in duplicates. *C)* IP3 levels were measured before and after stimulation with TNP-BSA. Samples were collected at the indicated times. Means ± SD of three independent experiments performed in duplicates are presented. *D–F)* Calcium response in Fluo-3- and Fura-Red-loaded cells. The cells were pretreated (dash-dot line) or not (solid line) with gangliosides, sensitised with IgE (*D* and *E*) or not (*F*), and stimulated in the presence (*D* and *F*) or absence (*E*) of extracellular calcium with TNP-BSA (1 μg/ml; *D* and *E*, arrow, antigen), or calcium ionophore A23187 (1 μg/ml; *F*, arrow A23). Fluorescence intensity was determined by flow cytofluorometry.

4.2.4. Formation of signalling assemblies in gangliosides-pretreated cells

Previously a simple method for determination of the subcellular translocations of signal transduction molecules was described [31]. The method is based on a gentle release of free cytoplasmic components after permeabilisation of the cells with the cholesterol sequestering reagent saponin, followed by complete solubilisation of all membrane components, including lipid rafts, by the detergent NP40. Using a modified version of this method we first compared the subcellular distribution of PLCγ2 and its phosphorylated form, in both control and gangliosides-pretreated cells.

The data presented in Figure 8*A* indicate that FcεRI aggregation in saponin permeabilised cells is followed by a rapid and transient increase in the amount of tyrosine phosphorylated PLCγ2 (arrow) and associated proteins. The observed change was in part due to an increased amount of insoluble PLCγ2 remaining in permeabilised cells, as demonstrated by immunoblotting with anti-PLCγ2 antibody. Pretreatment with gangliosides of saponin permeabilised cells reduced the amount of tyrosine phosphorylated PLCγ2 and coimmunoprecipitated proteins. This effect was in part related to a decrease in the amount of insoluble PLCγ2 and was most profound 5 min after antigen triggering. Because of the observed changes in cellular morphology and the decreased amount of F-actin in gangliosides-pretreated cells, we also analysed the tyrosine phosphorylation of ezrin, which functions as an intermediate between the actin cytoskeleton and integral plasma membrane proteins [32]. Although the amount of ezrin bound to permeabilised control cells (-Ga) did not show any significant change in the course of cell activation, its tyrosine phosphorylation was dramatically increased 30 s after activation, and then declined. Pretreatment with gangliosides decreased the amount of ezrin in saponin permeabilised cells. Interestingly, the background level of tyrosine phosphorylated ezrin (0 min) was higher in gangliosides pretreated cells than in control cells, and FcεRI aggregation resulted in a decreased tyrosine phosphorylation of ezrin in gangliosides-pretreated cells (Figure 8*B*). Finally, we investigated the distribution of Akt, which is recruited to the plasma membrane in activated cells by virtue of its interaction with PIP3 and phosphatidylinositol 3,4-bisphosphate [33]. In control cells (-Ga) the amount of tyrosine phosphorylated Akt in saponin permeabilised cells increased during FcεRI activation (Figure 8*C*). However, this increase was due not only to an augmentation of Akt tyrosine phosphorylation, but was mainly attributable to an increased association of Akt with insoluble material in saponin permeabilised cells, as

indicated by anti-Akt immunoblotting. In gangliosides-pretreated cells, both Akt tyrosine phosphorylation and its association with insoluble material were reduced.

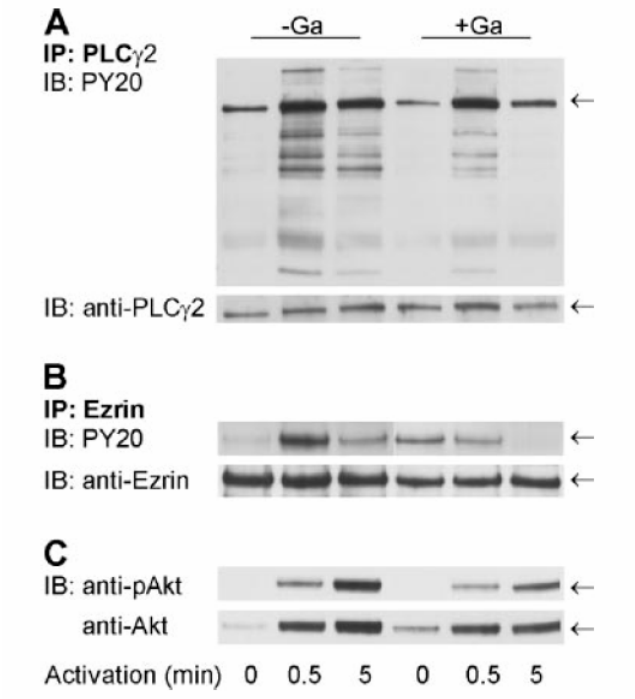

Figure 8: Decreased formation of PLCγ2-, Ezrin- and Akt-containing signalling assemblies in gangliosides-pretreated cells. RBL-2H3 cells were incubated with isolated brain gangliosides in G-medium (+Ga) or in G-medium alone (-Ga), sensitised with IgE, and activated with TNP-BSA (1 µg/ml). After the indicated time intervals, the cells were spun down and resuspended in permeabilisation buffer containing 0,1 % saponin, followed by centrifugation and extraction of the "empty" cells with NP40. The insoluble material (nuclei and cytoskeleton) was removed by centrifugation and the supernatant immunoprecipitated with anti-PLCγ2-coated protein A beads (*A*) or anti-ezrin-coated protein G beads (*B*) before SDS-PAGE and immunoblotting with anti-phosphotyrosine antibody (PY20). Alternatively, the supernatant was directly analysed by SDS-PAGE and immunoblotting with anti-phospho-Akt (pAkt) antibody (*C*). After stripping, the membranes were tested for the presence of PLCγ2, ezrin, and Akt with the corresponding antibodies. Arrows in *A*, *B*, and *C* indicate, respectively, positions of PLCγ2, ezrin and Akt.

5. Conclusion

Carcinoembryonic cell adhesion molecule 1 (CEACAM1) is a human membrane glycoprotein. At the first part of this thesis we describe method for isolation of CEACAM1 glycoprotein from bile and characterise its efficiency and recovery. We used affinity chromatography with immobilised monoclonal anti-CEA F34-187 antibodies. This method based on the oxidation of the immunoglobulin carbohydrate component located on the Fc fragment of antibody by periodate and oriented bounding to hydrazide-derivated matrix. Crude protein fraction obtained from bile by TCA precipitation was applied onto the affinity column and CEACAM1 was eluted with 6 M guanidine-HCl. A single immunopositive 85 kDa band of CEACAM1 was detected on the western blot with anti-CEA antibody. Probably due to the high glycosylation of CEACAM1 any common method of protein staining was not applicable except staining with lectin.

The second part describes an effect of exogenous gangliosides on signalling of mast cells. Gangliosides released from tumour cells, as well as administered exogenously, suppress the immune responses by largely unknown mechanisms. We show here that a pretreatment of rat basophilic leukaemia cells (RBL-2H3) with isolated brain gangliosides inhibited the release of preformed secretory mediators (β-glucuronidase) from cells activated via FcεRI but not via Thy-1 glycoprotein. Exogenously administered gangliosides also affected the cell-substrate adhesion and the levels of polymeric filamentous actin (F-actin) in antigen-activated cells. Although the production of phosphoinositides was also decreased, enzymatic activity of phosphatidylinositol 3-kinase (PI3K) was not inhibited. Gangliosides had no or only marginal effect on the association of aggregated FcεRI with glycosphingolipid-enriched membranes (GEM) and on tyrosine phosphorylation of FcεRI. Though pretreatment with gangliosides did not inhibit the association of LAT with phospholipase C (PLCγ1 and PLCγ2), but tyrosine phosphorylation of these enzymes, as well as their enzymatic activities and association with detergent-insoluble signalling assemblies were reduced. This resulted in a decreased production of inositol 1,4,5-trisphosphate (IP3) and an inhibition of Ca^{2+} mobilisation. The combined data support the concept that exogenously administered gangliosides interfere with those properties of GEM that are important for the formation of plasma membrane-associated signalling assemblies containing PLCγ but not for initial tyrosine phosphorylation of FcεRI subunits.

6. Abbreviations

BSA	bovine serum albumin
BSS	20 mM HEPES (pH 7,4), 135 mM NaCl, 5 mM KCl, 1,8 mM $CaCl_2$, 1 mM $MgCl_2$ a 5,6 mM glucose
$[Ca^{2+}]_i$	concentration of free intracellular Ca^{2+}
CEA	carcinoembryonic antigen
CEACAM1	carcinoembryonic antigen cell adhesion molecule 1
EDTA	ethylendiamintetraacetic acid
F-actin	polymeric filamentous actin
FcεRI	high affinity IgE receptor
GEM	glycosphingolipid-enriched membrane domain
G-medium	1:1 RPMI 1640 a MEM (minimum essential medium) with 1 mM natrium pyruvat and 3 mM L-glutamine, penicillin (100 U/ml), streptomycin (100 μg/ml), D-glucose (2,5 mg/ml) and 1 % (v/v) fetal calf serum.
GM1	monosialogangliosid, $II^3NeuAcGgOse_4Cer$
GD1a	disialogangliosid, $IV^3NeuAc\ II^3NeuAcGgOse_4Cer$
GT1b	trisialogagliosid, $IV^3NeuAc\ II^3\ (NeuAc)_2GgOse4Cer$
GPI	glycosyl-phosphatidylinositol
HEPES	N-2-hydroxyethylpiperazin-N´-ethansulfonic acid
HRP	horseradish peroxidase
IP	immunoprecipitation
IP3	inositol 1,4,5-triphosphate
LAT	linker for activation of T cells
mAb	monoclonal antibody
NP40	Nonidet-P40
PBS	phosphate buffered saline: 80 mM Na_2HPO_4, 20 mM NaH_2PO_4, 100 mM NaCl; pH 7,4
PI3K	phosphatidylinositol 3-kinase
PIP2	phosphatidylinositol 4,5-bisphosphate
PLCγ1, PLCγ2	phospholipase C, isoforms γ1 a γ2

PMSF	phenylmethylsulfonylfluorid (inhibitor of serine proteases)
PTK	protein tyrosinkinase
PY20	anti-phosphotyrosine antibody
SDS-PAGE	sodium dodecyl sulphate- polyacrylamide gel electrophoresis
TLC	thin-layer chromatography
TNP	2,4,6-trinitrophenyle
Tris-HCl	2-amino-2-(hydroxymethyl)-1,3-propandiol hydrochloride
Triton X-100	t-octylphenoxypolyethoxyethanol, non-ionic detergent
Tween 20	polyoxyethylene sorbitan monolaurate, non-ionic detergent

7. List of author´s publications

Publications:

1. Dráberová, L., Dudková, L., Boubelík, M., Tolarová, H., Šmíd, F. and Dráber, P.: Exogenous administration of gangliosides inhibits FcεRI-mediated mast cell degranulation by decreasing the activity of phospholipase Cγ. *J. Immunol.* (2003), **171**: 3585-3593. (IF = 6,702)
2. Muchová, L., Jirsa, M., Kuroki, M., Dudková, L., Beneš, M. J., Mareček, Z. and Šmíd, F.: Immunoaffinity isolation of CEACAM1 on hydrazide-derivated cellulose with immobilised monoclonal anti-CEA antibody. *Biomed. Chromatogr.* (2001), **15**: 418-422. (IF = 1,432)
3. Tesař, V., Jančová, E., Dudková, E., Jirsa, M. Jr.,. Zima, T., Merta, M., Žabka; J.: Urinary 8-Isoprostane and IL-6/EGF in primary and secondary glomerulonephritides (anca-positive renal vasculitis, lupus nephritis, IGA nephropathy and membranous nephropathy). *Cardionephrology* (2000), **6**: 321-324.
4. Rychlík, I., Tesař, V., Dudková, L., Pacltová, M., Jirsa, M.: IgA nephropathy and oxidative stress during fish oil treatment. *Cardionephrology* (2000), **6**: 505-506.

Abstracts:

1. Kráslová, I., Muchová, L., Vítek, L., Brůha, R., Stříteský, J., Svatošováa, J., Švestka, T., Novotný, A., Subhanová, I., Dudková, L.: The Dynamic changes in cytokine profiles of patients with Ticlopidin induced cholestatic hepatitis and their correlation with biochemical markers of liver damage. *J. Hepatol.* (2004), **40**:174.
2. Rychlík, I., Tesař, V., Dudková, L., Pacltová, M., Jirsa, M.: Oxidative stress in IgA nephropathy during fish oil treatment. *J. Am. Soc. Nephrol.* (2000), **11**: 76A.
3. Merta, M., Reiterová, J., Žabka, J., Ryšavá, R., Dudková, L., Jáchymová, M., Tesař, V.: Plasmatický endothelin a koncentrace vybraných prostanoidů v moči u polycystické choroby ledvin autosomálně dominantního typu (PCHLAD). *Aktuality v nefrologii* (2000), **1**: 28.
4. Rychlík, I., Tesař, V., Jirsa, M., Pacltová, M., Dudková, L.: Levels of some urinary eicosanoids and serum interleukins during fish oil treatment in IgAN. *Blood Purif.* (1999), **17**: 229.

8. References

[1] Prall, F., Nollau, P., Neumaier, M., Haubeck, H. D., Drzeniek, Z., Helmchen, U., Löning, T., Wagener, C.: CD 66a (BGP), an adhesion molecule of the carcinoembryonic antigen family, is expressed in epithelium, endothelium, and myeloid cells in a wide range of normal human tissues. *J. Histochem. and Cytochem.* (1996), **44**: 35-41.

[2] Huang, J., Hardy, J. D., Sun, Y. and Shively, J. E.: Essential role of biliary glycoprotein (CD66a) in morphogenesis of the human mammary epithelial cell line MCF10F. *J. Cell Sci.* (1999), **112**: 4193-4205.

[3] Iijima, H., Neurath, M. F., Nagaishi, T., Glickman, J. N., Nieuwenhuis, E. E., Nakajima, A. et al.: Specific regulation of T helper cell1-mediated murine colitis by CEACAM1. *J. Exp. Med.* (2006), **199**: 471-482.

[4] Hammarström, S.: The carcinoembryonic antigen family: structures, suggested functions and expression in normal and malignant tissues. *Canc. Biol.* (1999), **9**: 67-81.

[5] Jirsa, M., Muchová, L., Dráberová, L., Dráber, P., Šmíd, F., Kuroki, M., Mareček, M. and Groen, A., K.: Carcinoembryonic antigen-related cell adhesion molecule 1 is the 85-kilodalton pronase resistant biliary glycoprotein in the cholesterol crystallization promoting low density protein-lipid complex. *Hepatology* (2001), **34**: 1075-1082.

[6] Svenberg, T., Wahren, B., Hammarström, S.: Elevated serum levels of a biliary glycoprotein (BGP I) in patients with liver or biliary tract disease. *Clin. Exp. Immunol.* (1979), **36**: 317-325.

[7] Neumaier, M., Fenger, U., Wagener, C.: Monoclonal antibodies for carcinoembryonic antigen (CEA) as a model system: identification of two novel CEA-related antigens in meconium and colorectal carcinoma tissue by western blots and differential immunoaffinity chromatography. *J. Immunol.* (1985), **135**: 3604-3609.

[8] Hakomori, S. and Igarashi, Y.: Functional role of glycosphingolipids in cell recognition and signaling. *J. Biochem. (Tokyo)* (1995), **118**: 1091-1103.

[9] Schwarzmann, G.: Uptake and metabolism of exogenou glycosphingolipids by cultured cells. *Semin. Cell. Dev. Biol.* (2001), **12**: 163-171.

[10] Simons, M., Friedrichson, T., Schulz, J. B., Pitto, M., Masserini, M. and Kurzchalia, T. V.**:** Exogenous administration of gangliosides displaces GPI-anchored proteins from lipid microdomains in living cells. *Mol. Biol. Cell* (1999), **10**: 3187-3196.

[11] Simons, K. and Toomre, D.: Lipid rafts and signal transduction. *Nat. Rev. Mol. Cell Biol.* (2000), **1**: 31-39.

[12] Kinet, J. P.: The high-affinity IgE receptor (FcεRI): From physiology to pathology. *Annu. Rev. Immunol* (1999), **17**: 931-972.

[13] Murakami, M., Kuroki, M., Arakawa, F., Kuwahara, M., Oikawa, S., Nakazato, H. and Matsuoka, Y.: A reference of the GOLD classification of monoclonal antibodies against carcinoembryonic antigen to the domain structure of the carcinoembryonic antigen molecule. *Hybridoma* (1995), **14**: 19-28.

[14] Laemmli, U. K.: Cleavage of structural proteins during the assembly of the head of bacteriophage T4. *Nature* (1970), **227**: 680-685.

[15] Towbin, H., Staehelin, T. and Gordon, J.: Electrophoretic transfer of proteins from polyacrylamide gels to nitrocellulose sheets: procedure and some applications. *Proc. Natl. Acad. Sci. USA* (1979), **76**: 4350-4354.

[16] Dráberová, L. and Dráber, P.: Functional expression of the endogenous Thy-1 gene and the transfected murine Thy-1.2 gene in rat basophilic leukemia cells. *Eur. J. Immunol.* (1991), **21**: 1583-1590.

[17] Surviladze, Z., Dráberová, L., Kubínová, L. and Dráber, P.: Functional heterogeneity of Thy-1 membrane microdomains in rat basophilic leukemia cells. *Eur. J. Immunol*. (1998), **28**: 1847-1858.

[18] Dráberová, L. and Dráber, P.: Crosss-linking of Thy-1 glycoproteins or high-affinity IgE receptors induces mast cell activation via different mechanisms. *Immunology* (1993), **80**: 103-109.

[19] Tolar, P., Dráberová, L. and Dráber, P.: Protein tyrosine kinase Syk is involved in Thy-1 signaling in rat basophilic leukemia cells. *Eur. J. Immunol.* (1997), **27**: 3389-3397.

[20] Halova, I., Draberova, L. and Draber, P.: A novel lipid raft-associated glycoprotein, TEC-21, activates rat basophilic leukemia cells independently of the type 1 Fc epsilon receptor. *Int. Immunol.* (2002), **14**: 213-223.

[21] Vlahos, C. J. and Matter, W. F.: Signal transduction in neutrophil activation. Phosphatidylinositol 3- kinase is stimulated without tyrosine phosphorylation. *FEBS Lett.* (1992), **309**: 242-248.

[22] Choi, O. H., Kim, J. H. and Kinet, J. P.: Calcium mobilization via sphingosine kinase in signalling by the Fc epsilon RI antigen receptor. *Nature* (1996), **380**: 634-636.

[23] Tatsuya, O., Masatoshi, H., Tanaka, A., Matsuda, H. et al.: IgE alone-induced actin assembly modifies calcium signaling and degranulation in RBL-2H3 mast cells, *Am J Physiol. Cell Physiol.* (2004), **286**: C256-263.

[24] Kovárová, M., Tolar, P., Arudchandran, R., Dráberová, L., Rivera, J. and Dráber, P.: Structure-function analysis of Lyn kinase association with lipid rafts and initiation of early signaling events after Fcε receptor I aggregation. *Mol. Cell Biol.* (2001), **21**: 8318-8328.

[25] Tolar, P., Dráberová, L., Tolarová, H. and Dráber, P.: Positive and negative regulation of Fcε receptor I-mediated signalling events by Lyn kinase C-terminal tyrosine phosphorylation. *Eur. J. Immunol*. (2004), **34**: 1136-1145.

[26] Howard, T. H. and Meyer, W. H.: Chemotactic peptide modulation of actin assembly and locomotion in neutrophils. *J. Cell Biol.* 1984. **98**: 1265-1271.

[27] Inabe, K., Ishiai, M., Scharenberg, A. M., Fresheney, N., Downward, J. and Kurosaki, T.: Vav3 modulates B cell receptor responses by regulating phosphoinositide 3-kinase activation. *J. Exp. Med.* (2002), **195**: 189-200.

[28] Barker, S. A., Caldwell, K. K., Pfeiffer, J. R. and Wilson, B. S.: Wortmannin-sensitive phospohorylation, translocation, and activation of PLCγ1, but not PLCγ2, in antigen-stimulated RBL-2H3 mast cells. *Mol. Biol. Cell*. (1998), **9**: 483-496.

[29] Field, K. A., Holowka, D. and Baird, B.: Compartmentalised activation of the high affinity immunoglobulin E receptor within membrane domains. *J. Biol. Chem.* (1997), **272**: 4276-4280.

[30] Barker, S. A., Caldwell, K. K., Hall, A., Martinez, A. M., Pfeiffer, J. R., Oliver, J. M. and Wilson, B. S.: Wortmannin blocks lipid and protein kinase activities associated with PI 3-kinase and inhibits a subset of responses induced by FcεR1 cross-linking. *Mol. Biol. Cell* (1995), **6**: 1145-1158.

[31] Dráberová, L., Amoui, M. and Dráber, P.: Thy-1-mediated activation of rat mast cells: the role of Thy-1 membrane microdomains. *Immunology* (1996), **87**: 141-148.

[32] Bretscher, A.: Regulation of cortical structure by the ezrin-radixin-moesin protein family. *Curr. Opin. Cell. Biol.* (1999), **11**: 109-116.

[33] Thomas, C. C, Deak, M., Alessi, D. R. and van Aalten M. F.: High-resolution structure of the Pleckstrin homology domain of protein kinase B/Akt bound to phosphatidylinositol (3,4,5)-trisphosphate. *Curr. Biol.* (2002), **12**: 1256-1262.